Critical dynamics of the two-dimensional random-bond Potts model with nonequilibrium Monte Carlo simulations

Shuangli Fan and Fan Zhong*

State Key Laboratory of Optoelectronic Materials and Technologies, School of Physics and Engineering, Zhongshan University, Guangzhou 510275, People's Republic of China

(Received 24 July 2008; revised manuscript received 15 November 2008; published 22 January 2009)

We study two-dimensional q-state random-bond Potts models for both $q=8$ and $q=5$ with a linearly varying temperature. By applying a successive Monte Carlo renormalization group procedure, both the static and dynamic critical exponents are obtained for randomness amplitudes (the strong to weak coupling ratio) of $r_0=3$, 10, 15, and 20. The correlation length exponent ν increases with disorder from less than to larger than unity and this variation is justified by the good collapse of the specific heat near the critical region. The specific heat exponent is obtained by the usual hyperscaling relation $\alpha=2-d\nu$ and thus indicates no possibility of the activated dynamic scaling. Both r_0 and q have effects on the critical dynamics of the disordered systems, which can be seen from variations of the rate exponent, the hysteresis exponent, and the dynamic critical exponent. Implications of these results are discussed.

DOI: 10.1103/PhysRevE.79.011122 PACS number(s): 05.50.+q, 75.50.Lk, 05.10.Ln, 75.40.Gb

I. INTRODUCTION

Impurities can have drastic effects on first-order phase transitions. In the late 1970s it was suggested that the addition of quenched impurities to a system undergoing a first-order phase transition would soften the transition to be continuous [1], which was then rigorously proved [2,3]. For two-dimensional (2D) disordered systems, arbitrarily small amount of disorder can soften the first-order transition to be continuous [3]. While for the system in three dimensions, there is a tricritical point [4–11] separating first-order and randomness-induced second-order phase transitions. However, the rounding of the first-order phase transition is not so well studied as that of the second-order one, which can be understood well by the Harris criterion [12]. The identification of universality classes in disordered systems whose pure versions have first-order phase transitions has thus been a focus and the determination of both the static and dynamic critical exponents is an important way to understand it.

The Potts model [13] in two or three dimensions is very appropriate for such study, for it exhibits a temperature-driven first-order phase transition when the state number $q>4$ in two dimensions or $q>2$ in three dimensions [14]. Up to now, there has been a lot of work on the random-bond Potts model, especially in two dimensions [4,15–25]. As the first large scale Monte Carlo simulation on the two-dimensional random-bond Potts model, the randomness-induced second-order phase transition was confirmed [15]. The critical exponents obtained by a finite-size scaling analysis [15] were in agreement with those of the two-dimensional Ising model and there were agreements on this scenario [16,17]. Also there were arguments that the induced second-order phase transition was controlled by a random fixed point [18,19] and the critical exponents were different from those of the two-dimensional Ising model [4]. In Ref. [4], a transfer matrix method was used and the results indicated a q dependence of β/ν and a weakly varying ν around unity. Monte Carlo simulations produced similar conclusions about the variations of β/ν and ν [20–25]. In numerical simulations the obtained exponents were to some extent dependent on the disorder strength (see, e.g., Ref. [25]), a dependence which was attributed to the crossover effects due to the pure and/or percolation fixed points and it was suggested that a disorder strength of $r_0=8-20$ was preferred to detect the random fixed point [23,26–29]. Here we will study the possible influence of the disorder strength on the critical exponents of the two-dimensional random-bond Potts model using a nonequilibrium method that can avoid critical slowing down.

In contrast to the statics, studies on the critical dynamics of the two-dimensional random-bond-induced second-order phase transition are fewer and the methods are restricted to finite-size scaling [30,31] and short-time dynamics [25,32,33]. In addition to a finite size scaling analysis with the Swendsen-Wang cluster algorithm [34] which showed that the dynamic critical exponent z of the two-dimensional random-bond eight-state Potts model was approximately equal to zero [30] in agreement with that of the two-dimensional Ising model [35], z was estimated with the short-time dynamic approach using the single spin-flip algorithm [25,33] to be greater than 2.17 [36] and to increase with the randomness amplitude [25]. The dynamic finite-size scaling analysis of the relaxation times of the two-dimensional random-bond Potts model with OY self-dual distribution suggested by Olson and Young [20] gave $z=3.76(4)$ for $q=24$ [31], which is compatible with $z=3.41(6)$ for $q=8$ obtained by the short-time dynamic approach [32]. As only two kinds of method have been used to study the critical dynamics and there is no systematic study on the q dependence of z, we will use the Monte Carlo renormalization group (MCRG) method to study the critical dynamics of the two-dimensional random-bond Potts model. In view of the successful extension of the weak universality hypothesis [37] to the critical dynamics in pure systems [36,38], we will study in this work the dynamic universality

*Corresponding author; stszf@mail.sysu.edu.cn

class in disordered systems under a wider range of randomness amplitude for different Potts state number q.

In conventional critical dynamics, the relaxation time τ diverges with the system size L as $\tau \sim L^z$. For disorder-driven continuous transitions, there is a possible activated dynamics [39] proposed originally for the random-field Ising model whose transition is suggested to be controlled by the zero temperature fixed point. For a system exhibiting the activated dynamics, it is the logarithm of the relaxation time that diverges with the power law of the system size. An additional exponent θ is introduced and the modified hyperscaling relation is $(d-\theta)\nu=2-\alpha$. For the q-state Potts model with quenched random impurities, an asymptotically exact mapping to the random-field Ising model was proposed for large q and possible activated dynamics was anticipated [4,26]. This possibility was checked by the scaling of the equilibrium relaxation times of the two-dimensional random-bond Potts model and the conventional dynamic scaling was found instead, albeit with some subtleties [31]. In this paper we shall present the dynamic scaling form of the specific heat as a test of the possible modified hyperscaling relation.

The method of this work is the dynamic MCRG in the presence of a linearly varying temperature. The renormalization group theory [40] and its combination with Monte Carlo simulations [41,42] are very powerful in studying critical phenomena. By matching correlation functions at different blocking levels at different times, the dynamic exponent z was obtained with the dynamic successive MCRG method [43,44]. The extended dynamic MCRG method used here and its field theoretical version have been proved to be very powerful in detecting both continuous and first-order phase transitions [38,45–47]. A linearly varying magnetic field was used to study the scaling of hysteresis of the disordered Ising model [48]. The linearly varying temperature acts as a driving force so that the critical slowing down induced by the randomness in such nonequilibrium situations can be greatly reduced, though the usual Metropolis algorithm is used.

The layout of the rest of the paper is as follows. The model and the method will be given in Sec. II. The disorder strength used ranges from $r_0=3$ to $r_0=20$. Section III presents the main results of this work. First presented are the estimations of the rate exponent r [45], the correlation length exponent ν, the hysteresis exponent $1/r\nu$, and the dynamic critical exponent z. The effects of both q and r_0 on these exponents are revealed. Then we determine the order parameter exponent β by the dynamic scaling form. Furthermore, good collapse of the rescaled specific heat near the critical region seems to indicate that the conventional critical dynamics still hold and no θ is necessary in the present cases. Finally we discuss the effects of the dynamic MCRG approach on the estimates of the critical exponents and the implication of our results. A summary is given in Sec. IV.

II. MODEL AND METHOD

The Hamiltonian of the random-bond Potts model is $H=-\Sigma_{\langle i,j\rangle}K_{ij}\delta_{\sigma_i\sigma_j}$, where δ is the Kronecker δ function and $\langle i,j\rangle$ denotes the sum over nearest-neighbor spin pairs. The spin variable σ_i of this model can take q different values and the interaction strength K_{ij} can take two different values, K_1 and K_2, with probability p and $1-p$. $r_0=K_1/K_2$ indicates the randomness amplitude of the system. We consider here the self-dual system, i.e., $p=0.5$, the exact transition coupling of which is determined by $(e^{K_1^c}-1)(e^{K_2^c}-1)=q$ [49].

The order parameter, the specific heat per site, and the nearest-neighbor correlation function are defined as

$$\langle M\rangle = (qN_{\max}/N-1)/(q-1), \tag{1}$$

$$C = \frac{L^d}{T^2}(\langle E^2\rangle - \langle E\rangle^2), \tag{2}$$

$$G_{nn} = \left\langle \frac{1}{dN}\sum_{\langle i,j\rangle}\delta_{\sigma_i\sigma_j}\right\rangle - \langle M\rangle^2. \tag{3}$$

Here $N_{\max}=\max(N_1,N_2,\ldots,N_q)$, N_q denotes the number of spins in state q, N the total number of spins, and E the energy per site.

We use dynamic MCRG to study the Potts model in the presence of a varying temperature $T=Rt$, where t is the time measured by Monte Carlo steps and R is the sweep rate of the temperature. Relations between the renormalized and unrenormalized quantities are

$$(T-T_c)^{(1)} = (T-T_c)b^{1/\nu} \tag{4}$$

and

$$R^{(1)} = Rb^r, \tag{5}$$

where b is the scaling factor and the superscript 1 indicates the first iteration of the renormalization procedure.

The exponents r and ν are obtained by matching the correlation functions of two blocked spin systems with the same size (the large lattice is renormalized one more time than the small one) in order to reduce the size effect. One can then obtain

$$r = \ln(R_s^{(m)}/R^{(m)})/\ln b \tag{6}$$

and

$$\nu = \ln b/\ln[(T_{ps}{}^{(m)}-T_c)/(T_p{}^{(m)}-T_c)], \tag{7}$$

where the subscript s indicates the small lattice.

For a second-order phase transition, the time scale of a finite system in the critical region is proportional to L^z. So we have $(t-t_c)^{(1)}=(t-t_c)b^{-z}$, where t_c is the time at which $T=T_c$. Combining this equation with Eqs. (4) and (5), and $T=Rt$, we obtain the scaling relation

$$1/\nu = r-z, \tag{8}$$

the validity of which has been confirmed [38,46,47].

III. NUMERICAL RESULTS

In this paper the dynamic MCRG procedure is carried on the two-dimensional random-bond Potts models for $q=8$ and $q=5$ and the lattice sizes are 512×512 and 256×256. The randomness amplitudes are $r_0=3$, 10, 15, and 20. The sweep

TABLE I. The exponents for the two-dimensional eight-state random-bond Potts model with several randomness amplitudes.

		$m=1$				$m=2$				$m=3$				$m=4$			
r_0	R	r	ν	$1/r\nu$	z	r	ν	$1/r\nu$	z	r	ν	$1/r\nu$	z	r	ν	$1/r\nu$	z
3	1×10^{-5}	5.188	0.655	0.295	3.660	4.662	0.759	0.283	3.344	4.452	0.787	0.286	3.181	4.380	0.816	0.280	3.154
	3×10^{-5}	4.986	0.649	0.309	3.446	4.549	0.721	0.305	3.162	4.410	0.778	0.291	3.125	4.373	0.840	0.272	3.182
	5×10^{-5}	4.857	0.646	0.319	3.310	4.451	0.717	0.313	3.057	4.335	0.743	0.310	2.990	4.280	0.780	0.299	2.998
	7×10^{-5}	4.834	0.649	0.319	3.294	4.443	0.709	0.318	3.032	4.322	0.733	0.316	2.958	4.146	0.803	0.300	2.900
	1×10^{-4}	4.787	0.645	0.324	3.237	4.446	0.698	0.323	3.012	4.350	0.714	0.322	2.949	4.324	0.753	3.3.7	2.996
10	1×10^{-5}	6.018	0.950	0.175	4.964	5.661	0.983	0.180	4.644	5.571	1.062	0.169	4.630	5.512	1.074	0.169	4.581
	3×10^{-5}	5.772	0.972	0.178	4.743	5.526	1.045	0.173	4.569	5.489	1.050	0.174	4.537	5.521	1.017	0.178	4.537
	5×10^{-5}	5.655	0.946	0.187	4.598	5.423	0.982	0.188	4.405	5.424	0.989	0.186	4.413	5.385	1.036	0.179	4.420
	7×10^{-5}	5.588	0.945	0.189	4.530	5.374	1.004	0.186	4.377	5.382	0.971	0.191	4.353	5.311	1.041	0.181	4.350
	1×10^{-4}	5.502	0.954	0.191	4.454	5.319	0.990	0.190	4.309	5.364	1.001	0.186	4.365	5.140	1.068	0.182	4.204
15	1×10^{-5}	6.329	1.049	0.151	5.375	6.043	1.131	0.146	5.159	5.969	1.076	0.156	5.040	5.975	1.123	0.149	5.084
	3×10^{-5}	6.070	1.054	0.156	5.122	5.835	1.084	0.158	4.913	5.825	1.083	0.159	4.901	5.777	1.128	0.153	4.891
	5×10^{-5}	5.930	1.063	0.159	4.988	5.726	1.083	0.161	4.803	5.738	1.109	0.157	4.837	5.654	1.133	0.156	4.772
	7×10^{-5}	5.854	1.033	0.165	4.886	5.660	1.086	0.163	4.739	5.689	1.068	0.165	4.753	5.611	1.145	0.156	4.738
	1×10^{-4}	5.764	1.041	0.167	4.803	5.598	1.090	0.164	4.681	5.643	1.074	0.165	4.712	5.577	1.062	0.169	4.636
20	1×10^{-5}	6.507	1.118	0.138	5.613	6.203	1.203	0.134	5.372	6.160	1.156	0.141	5.294	6.030	1.168	0.142	5.174
	3×10^{-5}	6.251	1.129	0.142	5.365	6.007	1.176	0.142	5.156	5.813	1.189	0.145	4.972	5.932	1.224	0.138	5.115
	5×10^{-5}	6.106	1.115	0.147	5.209	5.918	1.155	0.146	5.053	5.919	1.199	0.141	5.086	5.666	1.257	0.140	4.871
	7×10^{-5}	6.033	1.129	0.147	5.147	5.849	1.151	0.149	4.980	5.872	1.140	0.149	4.995	5.667	1.202	0.147	4.835
	1×10^{-4}	5.925	1.107	0.153	5.022	5.771	1.128	0.154	4.885	5.781	1.150	0.150	4.911	5.647	1.206	0.147	4.818

rate of the large lattice ranges from 1×10^{-5} to 1×10^{-4} and that of the small lattice ranges from 1×10^{-5} to 2×10^{-1}. The number of samples for average varies from 200 to 10 000. In each run (sample), including every MCRG procedure, the numbers of K_1 and K_2, which are distributed randomly on the lattice, are kept equal so that the random fluctuations are suppressed.

A. Exponents estimates by the dynamic MCRG

Estimates of r, ν, $1/r\nu$, and z with the successive dynamic MCRG are listed in Table I for the two-dimensional eight-state Potts model, where results up to $m=4$ are presented. For each r_0, the temperature sweep rates in the second column are for the large lattice and the estimates of r, ν, $1/r\nu$, and z maintain almost constant after the first iteration as irrelevant variables are iterated away. But the sweep rate R is a relevant variable (see Table I), further iterations lead to the scattering of estimates of those exponents again (not shown in Table I). The smaller sweep rates lead the system to be more equilibriumlike and closer to the fixed point and more accurate estimations are expected if considerable samples are used [38]. We get averages over $m=2$ to $m=4$ as shown in Table III, where in the parentheses are given standard deviations from the averages only: Errors arising from the numerical renormalization procedures have not been taken into account. The rate exponent r increases with r_0, which means a wider sweep rate range is needed for the small lattice. The increasing of z with r_0 indicates stronger critical slowing down and the decreasing of $1/r\nu$ indicates more severe hysteresis. It should be noted that the correlation length exponent estimated here is around unity for $r_0=10$, very close to that of the 2D pure Ising model. With even larger randomness amplitude, however, our estimations of the exponent ν go beyond unity. The inequality of $\nu\geqslant 2/d$ for the randomness-induced phase transitions [50] is thus satisfied when the randomness amplitude $r_0\geqslant 10$. We shall come back to these results in the discussion section below.

To see the q dependence of these exponents, we carry all these calculations on the two-dimensional five-state Potts model, the pure version of which exhibits a weak first-order transition. The lattice sizes and the range of the sweep rates are the same as those of the $q=8$ Potts model. Results are listed in Table II and the corresponding averages are shown in Table III. For clarity, we plot variations of r, ν, $1/r\nu$, and z with r_0 for both $q=8$ and $q=5$ in Figs. 1(a)–1(d), which show clearly that the varying trends of the estimations with the randomness amplitude for $q=5$ are similar to those for $q=8$. When $r_0\geqslant 10$, the q dependence of ν is very weak, the hysteresis exponent $1/r\nu$ decreases with q, both the dynamic exponent z and the rate exponent r increase with q, which indicate that q is relevant to the critical dynamics.

B. Dynamic scaling forms of the order parameter

The dynamic scaling form of the order parameter is [51]

$$M(T-T_c,R)=R^{\beta/r\nu}f_1((T-T_c)R^{-1/r\nu}), \tag{9}$$

which has been testified for the pure systems. Here we will try to show its validity when quenched randomness is incor-

TABLE II. Critical exponents for the two-dimensional five-state random-bond Potts model with several randomness amplitudes.

		$m=1$				$m=2$				$m=3$				$m=4$			
r_0	R	r	ν	$1/r\nu$	z	r	ν	$1/r\nu$	z	r	ν	$1/r\nu$	z	r	ν	$1/r\nu$	z
3	1×10^{-5}	4.797	0.713	0.292	3.395	4.310	0.801	0.290	3.062	4.176	0.826	0.290	2.965	4.117	0.931	0.261	3.044
	3×10^{-5}	4.637	0.716	0.301	3.240	4.234	0.787	0.300	2.962	4.106	0.830	0.294	2.901	4.049	0.888	0.278	2.922
	5×10^{-5}	4.586	0.730	0.299	3.216	4.228	0.808	0.293	2.989	4.146	0.799	0.302	2.895	4.141	0.834	0.290	2.942
	7×10^{-5}	4.549	0.722	0.305	3.163	4.238	0.770	0.306	2.940	4.121	0.790	0.307	2.854	4.015	0.839	0.297	2.824
	1×10^{-4}	4.509	0.721	0.308	3.122	4.195	0.781	0.305	2.915	4.120	0.786	0.309	2.847	4.066	0.800	0.308	2.816
10	1×10^{-5}	5.660	0.962	0.184	4.621	5.269	1.040	0.183	4.307	5.196	1.029	0.187	4.224	5.192	1.064	0.181	4.252
	3×10^{-5}	5.511	0.982	0.185	4.493	5.182	1.030	0.187	4.211	5.154	1.032	0.188	4.185	5.118	1.002	0.195	4.120
	5×10^{-5}	5.414	0.946	0.195	4.357	5.116	1.010	0.194	4.126	5.106	1.015	0.193	4.120	5.146	1.007	0.193	4.153
	7×10^{-5}	5.352	0.961	0.194	4.311	5.093	1.012	0.194	4.104	5.080	1.008	0.195	4.088	5.069	1.076	0.183	4.139
	1×10^{-4}	5.292	0.947	0.200	4.236	5.054	1.008	0.196	4.062	5.049	1.008	0.196	4.057	5.030	1.057	0.188	4.084
15	1×10^{-5}	5.989	1.042	0.160	5.029	5.627	1.065	0.167	4.688	5.601	1.135	0.157	4.720	5.519	1.167	0.155	4.662
	3×10^{-5}	5.840	1.058	0.162	4.895	5.517	1.092	0.166	4.601	5.513	1.104	0.164	4.607	5.366	1.171	0.159	4.512
	5×10^{-5}	5.707	1.047	0.167	4.752	5.435	1.085	0.170	4.514	5.447	1.078	0.170	4.520	5.347	1.145	0.163	4.473
	7×10^{-5}	5.646	1.047	0.169	4.691	5.401	1.084	0.171	4.479	5.395	1.098	0.169	4.484	5.360	1.136	0.164	4.480
	1×10^{-4}	5.575	1.050	0.171	4.623	5.350	1.086	0.172	4.429	5.345	1.089	0.172	4.427	5.347	1.145	0.163	4.474
20	1×10^{-5}	6.226	1.089	0.148	5.308	5.836	1.114	0.154	4.938	5.816	1.197	0.144	4.980	5.820	1.191	0.144	4.981
	3×10^{-5}	6.006	1.139	0.146	5.128	5.734	1.159	0.151	4.871	5.713	1.223	0.143	4.895	5.511	1.177	0.154	4.662
	5×10^{-5}	5.908	1.106	0.153	5.004	5.641	1.188	0.149	4.799	5.617	1.188	0.150	4.775	5.487	1.265	0.144	4.696
	7×10^{-5}	5.834	1.124	0.153	4.944	5.583	1.177	0.152	4.734	5.575	1.155	0.155	4.709	5.527	1.170	0.155	4.672
	1×10^{-4}	5.742	1.122	0.155	4.850	5.521	1.159	0.156	4.658	5.519	1.172	0.155	4.666	5.334	1.189	0.158	4.493

porated and determine the static exponent β from the best data collapse of the order parameter with Eq. (9). The details of this method have been discussed in our previous work [38,46] and we only present the results here. From the best collapse in Figs. 2 and 3, where the estimations of $1/r\nu$ in Table III are used, estimations of β and hence β/ν are determined as shown in Table III. The errors of β are roughly determined by the ranges of conjectured β which can give similarly satisfactory data collapse of the order parameter by direct inspection. These ranges and hence the errors of β thus obtained are quite large compared with the errors of other quantities as can be seen from Fig. 1. But we keep them as we have not taken into account the errors of $1/r\nu$ in the estimations. The errors of β/ν are determined by those of β and ν by the error propagation. The dependence of these two exponents β and β/ν on q is pronounced, as shown in Figs. 1(e) and 1(f). Considering the errors of β and β/ν, one sees that, for each q, they appear to be nearly constant when $r_0 \geqslant 10$. With the two independent static exponents β and ν being determined, all the other static exponents can be calculated.

C. Dynamic scaling forms of the specific heat

Applying the estimations of ν in the preceding section to the conventional hyperscaling relation, we get the specific heat exponents which evolve from positive to zero and then negative when increasing r_0. In this section, we focus on the $q=8$ Potts model as an example to discuss the specific heat and its dynamic scaling form.

Applying the estimations of ν in Table III to the hyperscaling relation $\alpha=2-d\nu$, we get $\alpha=0.486(86)$, $-0.042(70)$,

TABLE III. Averages of the exponents obtained by the dynamic renormalization group approach.

r_0	q	r	ν	$1/r\nu$	z	β	β/ν
3	8	4.39(12)	0.757(43)	0.302(16)	3.07(12)	0.130(15)	0.172(10)
	5	4.15(8)	0.818(43)	0.295(13)	2.93(7)	0.128(10)	0.157(4)
10	8	5.43(13)	1.021(35)	0.181(7)	4.45(13)	0.170(20)	0.167(14)
	5	5.12(7)	1.027(23)	0.190(5)	4.15(7)	0.161(20)	0.157(16)
15	8	5.75(15)	1.098(27)	0.158(6)	4.84(15)	0.173(20)	0.158(14)
	5	5.44(10)	1.112(34)	0.167(5)	4.54(9)	0.164(20)	0.148(14)
20	8	5.88(17)	1.180(35)	0.144(5)	5.03(17)	0.176(20)	0.149(13)
	5	5.62(14)	1.182(34)	0.151(5)	4.77(14)	0.170(20)	0.144(13)

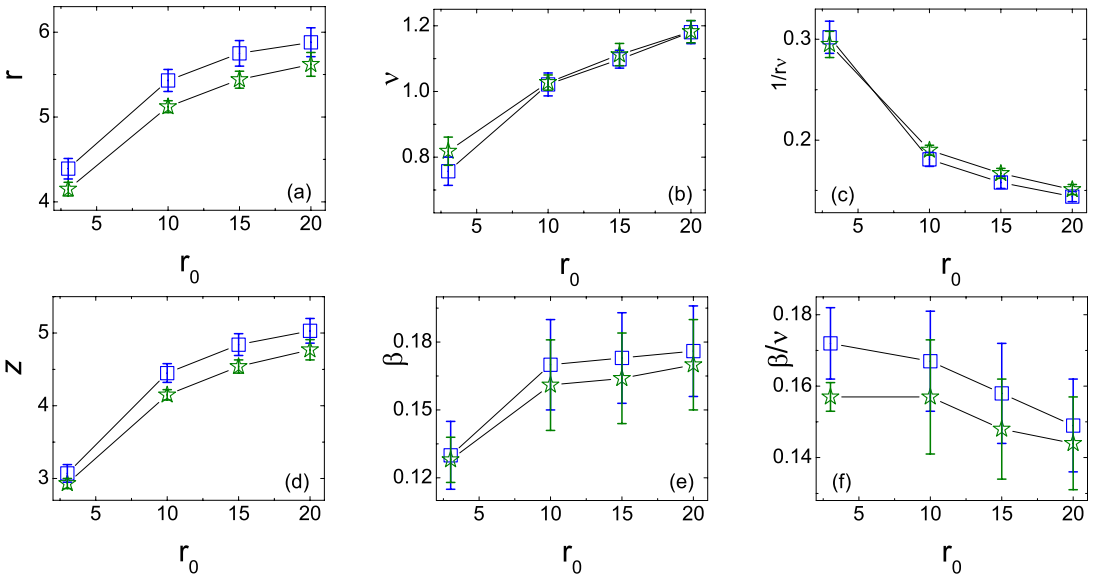

FIG. 1. (Color online) Variations of exponents with the randomness amplitude r_0 for $q=8$ (square) and $q=5$ (star).

−0.196(54), and −0.360(70) for $r_0=3$, 10, 15, and 20, respectively. For the specific heat having power-law dependence (with positive α) on the reduced temperature near the criticality, the dynamic scaling form is [51]

$$C(T-T_c,R) = R^{-\alpha/r\nu} f_2((T-T_c)R^{-1/r\nu}), \tag{10}$$

which has been testified for the pure systems. For $r_0=3$, we get positive α by the hyperscaling relation and the corresponding dynamic scaling form of the specific heat is shown in Fig. 4(a), which is quite good upon considering the variation of each curve, similarly to the pure case [38]. The negative specific heat exponent means, on the other hand, a finite cusp appears at the critical point and the dynamic scaling form is

$$C(T-T_c,R) = C_0 + R^{-\alpha/r\nu} f_3((T-T_c)R^{-1/r\nu}). \tag{11}$$

By seeking the most desirable collapsing as shown in Figs. 4(b)–4(d), C_0 can be determined, which are $C_0=16.5(5)$, 3.9(3), and 2.4(2), respectively. The increased randomness amplitude leads to stronger fluctuations, especially of the energy. For $r_0=20$ the fluctuations of the energy is so severe that more than 10 000 randomness realizations have been used to obtain the specific heat curves and the range of the sweep rate is from $R=0.000\,05$ to $R=0.001$. The desirable collapsing of the specific heat with different α obtained by the conventional hyperscaling relation $\alpha=2-d\nu$ suggests the conventional rather than activated dynamics at the criticality.

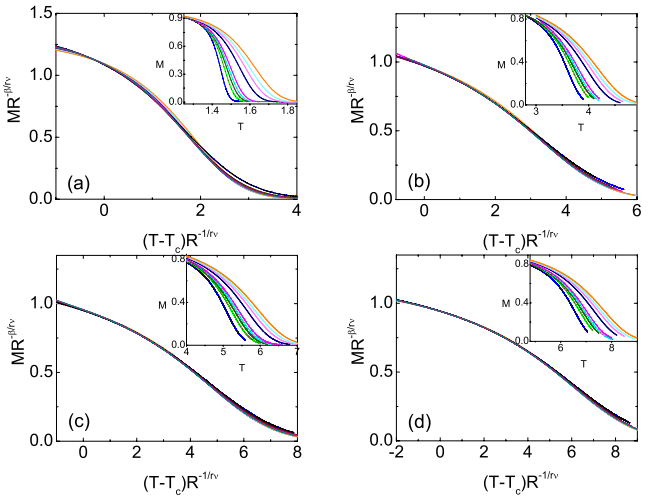

FIG. 2. (Color online) The dynamic scaling forms of the order parameter for the two-dimensional $q=8$ random-bond Potts model with $r_0=3$ (a), 10 (b), 15 (c), and 20 (d). Insets show the original curves for the large lattice (dashed lines) and the small lattice (solid lines). Sweep rates from left to right are 0.000 01, 0.000 03, 0.000 05, 0.000 07, and 0.0001 for the large lattice and 0.000 01, 0.000 03, 0.000 05, 0.000 07, 0.0001, 0.0003, 0.0005, 0.0007, and 0.001 for the small lattice.

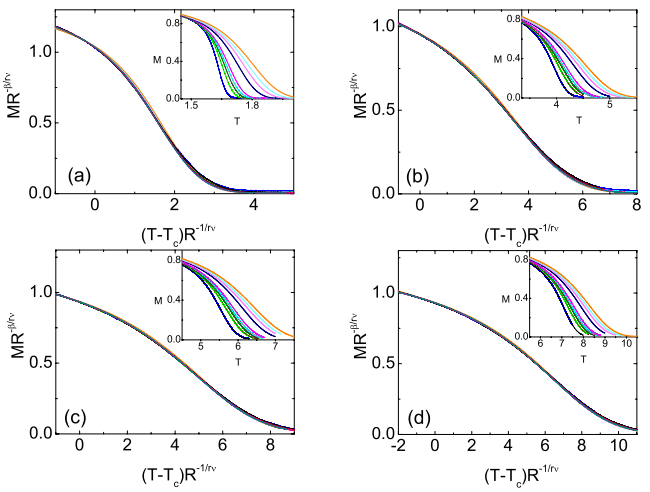

FIG. 3. (Color online) The same as Fig. 2 except that it is for the two-dimensional $q=5$ random-bond Potts model.

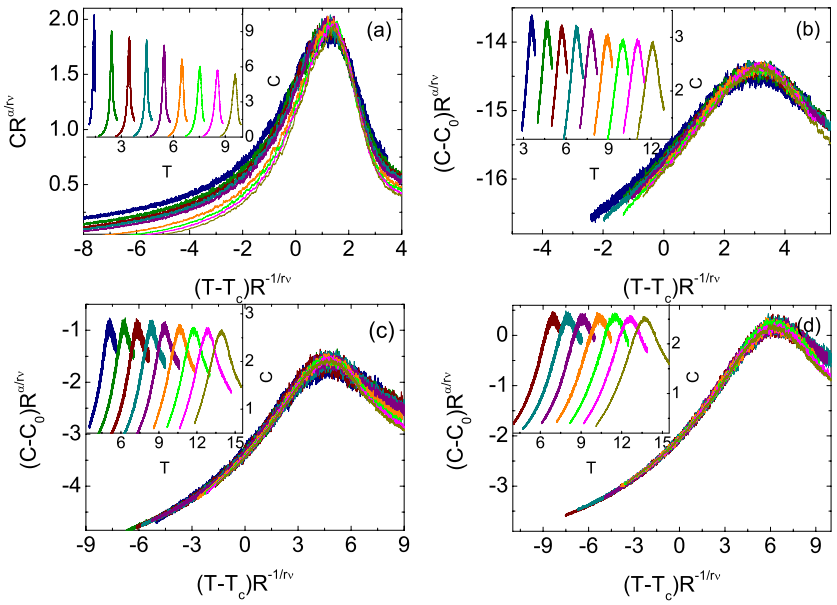

FIG. 4. (Color online) Dynamic scaling forms of the specific heat for $r_0=3$ (a), 10 (b), 15 (c), and 20 (d). Insets show the original curves. The sweep rates from left to right in (a)–(c) are 0.000 01, 0.000 03, 0.000 05, 0.000 07, 0.0001, 0.0003, 0.0005, 0.0007, and 0.001, respectively. While the sweep rates in (d) are from 0.000 05 to 0.001. Except for the first one, curves in each inset have been shifted along the horizontal coordinate for clarity.

For $r_0=10$, $\nu=1.021(35)$, which is around unity. If the specific heat were logarithmically divergent, i.e., $C\sim\ln L$, the corresponding dynamic scaling form should be

$$C(T-T_c,R)=-\frac{1}{r}f_4((T-T_c)R^{-1/r\nu})\ln R. \tag{12}$$

However, the specific heat curves do not collapse at all according to this equation, illustrated by Fig. 5(a). If a constant term $C_0\approx 2.3$ is added to the right-hand side of Eq. (12), the collapsing appears just around the peaks of the specific heat, as shown in Fig. 5(b).

IV. DISCUSSIONS

Table IV shows part of our results and those of Ref. [25] measured by the short-time dynamic approach for comparison and the agreement is very good. For $q=8$ with $r_0=10$, the estimate of ν around unity is consistent with those of Refs. [20,21]. The result of $\beta/\nu=0.160(4)$ for a large disorder strength [20] agrees quite well with $\beta/\nu=0.158(14)$ for $q=8$ with $r_0=15$ in Table III. While our estimate of $\beta/\nu=0.167(14)$ for $q=8$ with $r_0=10$ is a little larger than $\beta/\nu=0.153(3)$ in Ref. [21] but agrees within errors. For $q=5$ with $r_0=10$, the correlation length exponent ν was reported to be around unity [22], which is consistent with our result. Our estimate of $\beta/\nu=0.157(16)$ is larger than $\beta/\nu=0.146(1)$ in Ref. [22] but again agrees within errors. In addition, the conclusions of the weak q dependence of ν and pronounced q dependence of β/ν when $r_0\geqslant 10$, as shown in Figs. 1(b) and 1(f), agree well with the conclusions of Ref. [4]. These, therefore, show favorably the reliability of the exponents obtained.

Both the static and dynamic critical exponents in this paper depend on the disorder strength. Such dependence in dilute Ising systems was explained within the framework of the renormalization group to be caused by the limited system sizes which made the asymptotic scaling region unavailable [28,29]. Corrections to scaling were then taken into account in the three-dimensional diluted Ising model and impurity concentration independent critical exponents were obtained [52]. In this work the temperature sweep rate of the large lattice varies from $R=1\times10^{-5}$ to $R=1\times10^{-4}$ and our averages are over this range. On account of the small rates used and the good collapse of both the order parameter and the specific heat near the critical region, corrections to scaling

TABLE IV. The exponents calculated by the dynamic MCRG (present work) and the short-time dynamic approach (Ref. [25]) for the $d=2$, $q=8$ random-bond Potts model with randomness amplitude of $r_0=3$ and 10.

	r_0	$(d-2\beta/\nu)/z$	$\beta/\nu z$	$1/\nu z$	d/z	z	β/ν	$1/\nu$
Present work	3	0.539(28)	0.0560(10)	0.430(41)	0.652(26)	3.07(12)	0.172(10)	1.32(8)
Ref. [25]		0.552(2)	0.0560(4)	0.438(9)	0.669(8)	2.99(4)/3.01(2)	0.169(9)/0.169(2)	1.32(3)
Present work	10	0.374(17)	0.0375(20)	0.220(14)	0.449(13)	4.45(13)	0.167(14)	0.98(3)
Ref. [25]		0.369(1)	0.0343(2)	0.226(5)	0.428(6)	4.67(7)/4.57(2)	0.156(11)/0.157(2)	1.03(3)

TABLE V. Critical exponents for the two-dimensional eight-state random-bond Potts model with randomness amplitudes of $r_0=3$ and $r_0=20$. The lattice sizes are 128×128 and 64×64.

		$m=1$				$m=2$				$m=3$				$m=4$			
r_0	R	r	ν	$1/r\nu$	z	r	ν	$1/r\nu$	z	r	ν	$1/r\nu$	z	r	ν	$1/r\nu$	z
3	1×10^{-5}	5.183	0.663	0.291	3.675	4.615	0.730	0.297	3.245	4.430	0.804	0.281	3.186	4.307	0.859	0.270	3.143
	3×10^{-5}	4.982	0.649	0.309	3.441	4.552	0.706	0.311	3.135	4.423	0.758	0.298	3.104	4.277	0.825	0.284	3.064
	5×10^{-5}	4.885	0.657	0.312	3.362	4.423	0.720	0.314	3.033	4.309	0.764	0.304	3.000	4.175	0.899	0.266	3.063
	7×10^{-5}	4.845	0.640	0.322	3.283	4.419	0.691	0.328	2.971	4.294	0.715	0.326	2.895	4.677	0.706	0.303	3.260
	1×10^{-4}	4.782	0.647	0.323	3.236	4.440	0.690	0.327	2.989	4.294	0.743	0.314	2.947	4.245	0.758	0.311	2.925
20	1×10^{-5}	6.453	1.133	0.137	5.570	6.095	1.173	0.140	5.242	6.028	1.192	0.139	5.190	5.686	1.398	0.126	4.971
	3×10^{-5}	6.203	1.087	0.148	5.283	5.976	1.132	0.148	5.093	6.001	1.153	0.145	5.133	5.849	1.316	0.130	5.089
	5×10^{-5}	6.065	1.115	0.148	5.168	5.882	1.165	0.146	5.024	5.840	1.184	0.145	4.995	5.334	1.368	0.137	4.603
	7×10^{-5}	5.998	1.105	0.151	5.094	5.813	1.129	0.152	4.927	5.841	1.105	0.155	4.937	5.557	1.332	0.135	4.806
	1×10^{-4}	5.907	1.098	0.154	4.997	5.754	1.157	0.150	4.890	5.772	1.168	0.148	4.916	5.503	1.210	0.150	4.676

[53] should be small and the asymptotic scaling region may possibly be available. On the other hand, the larger r_0 and smaller R both lead to even stronger critical fluctuations and more independent samples are needed for averages, as we have done.

In Ref. [27] the crossover of the system from the pure and/or percolation fixed point to the random one was observed by increasing the lattice size. To test the possible size effects, we carry the dynamic renormalization group procedure again on the eight-state random-bond Potts model with $r_0=3$ and $r_0=20$, but the lattice pairs are now 128×128 and 64×64. More independent samples are used and estimations of the critical exponents are shown in Table V.

When $r_0=3$, the averages over $m=2$ to $m=4$ agree well with those in Table III both sets are listed in Table VI and thus the finite-size effects can be neglected. Fluctuations are very large when $r_0=20$. When $m=4$, the linear dimension of the large lattice is 8×8 and there are considerable statistical fluctuations. Consequently, we get averages only over $m=2$ and $m=3$ and compare them with the averages in Table III, as shown in Table VI. The estimations of each exponent agree with each other within statistical errors and so finite-size effects are slight if exists. In particular, there is no systematic finite-size effects even considering the slight differences in the numbers themselves: Though ν (for $r_0=3$) and r (for $r_0=20$) decrease a little, z (for $r_0=3$) and ν (for $r_0=20$) show an opposite trend (see Table VI). In fact, we match the correlation functions between systems with the same size and the finite-size effects should be small for our renormalization group method.

Having shown that the obtained exponents appear reliable, we now discuss their implication. The exponent ν goes beyond unity when $r_0\geqslant10$. We have shown that $\alpha=2-d\nu$ holds in Sec. III C and thus α is positive when $r_0<10$ and negative when $r_0\geqslant10$. According to the Harris criterion [12], this may therefore indicate that the disorder is relevant for $r_0<10$ and irrelevant for $r_0\geqslant10$. The distinct scaling forms of the specific heat displayed in Sec. III C also show clearly that there appear to be two distinct regimes that seem to agree with the scenario proposed in Ref. [4] of two fixed points, a pure one and a random one. However, the disorder of amplitude less than 10 is relevant. The agreement of all the exponents in this regime obtained by various methods seems they may not be just effective exponents that are affected by crossover between the pure and disordered one, but may also possibly indicate that each r_0 has its own fixed point. For the large disorder regime, disorder is irrelevant and there should be a random fixed point controlling the critical behavior. The critical exponents, in particular, should be independent of the disorder amplitude and identical in this regime. Though the exponents we obtained depends on r_0, they may still be regarded as nearly constant if the statistical errors are taken into account and thus may support a single random fixed point. The small variations in the exponents, having shown above not to be due to the finite-size effects as they are not systematically reduced, may be a result of the influence of the percolation fixed point. Further studies are still needed.

V. SUMMARY

We have studied the two-dimensional random-bond Potts model for both $q=8$ and $q=5$ with the dynamic MCRG approach. Effects of both the randomness amplitude r_0 and the states number q of the Potts model on the critical properties are investigated. The dynamic exponent z increases with q, which means slower and slower critical dynamics. The decreasing of $1/r\nu$ with q means even more severe hysteresis

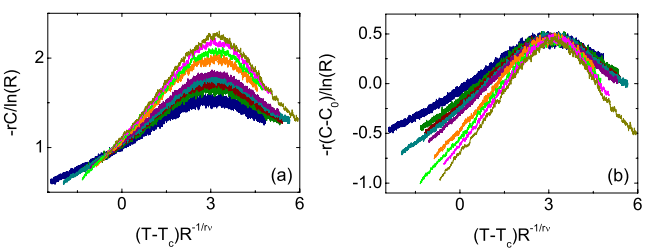

FIG. 5. (Color online) Rescaling of the specific heat for $r_0=10$ according to the logarithmically divergent dynamic scaling form.

TABLE VI. Averages of the exponents obtained by the dynamic renormalization group approach. "L" indicates the sizes of the lattice pairs.

r_0	L	r	ν	$1/r\nu$	z
3	128-64	4.39(14)	0.758(63)	0.302(20)	3.06(11)
	512-256	4.39(12)	0.757(43)	0.302(16)	3.07(12)
20	128-64	5.90(12)	1.156(27)	0.147(5)	5.03(12)
	512-256	5.88(17)	1.180(35)	0.144(5)	5.03(17)

due to the introduced temperature sweep rate. Thus, the weak universality class cannot be extended to the dynamics in such random-bond systems. Applying the estimated correlation length exponent ν to the hyperscaling relation $\alpha=2-d\nu$, we get specific heat exponent α varying with the randomness amplitude from positive to negative accordingly. This trend is verified by the dynamic scaling forms of the specific heat and the conventional dynamic scaling still holds in such random systems. Also, the logarithmic divergence of the specific heat with the disorder strength of $r_0=10$ is excluded in our work. The systematic dependence on the randomness of ν and α and the distinct behavior of the specific curves shown in Fig. 4 clearly indicate that there are two distinct regimes corresponding to low ($r_0 \lesssim 10$) and high ($r_0 \gtrsim 10$) randomness amplitudes, possibly in accordance to the two possible fixed points found in Ref. [4]. However, r_0 is clearly relevant when $r_0 \lesssim 10$ and each may give its own corresponding set of critical exponents, though crossover between the pure and random fixed point is also possible. When $r_0 \gtrsim 10$, r_0 is irrelevant and percolation fixed point possibly results in the impurity-dependent critical exponents.

ACKNOWLEDGMENTS

This work was supported by the NNSF of China (Grant No. 10625420).

[1] Y. Imry and M. Wortis, Phys. Rev. B **19**, 3580 (1979).
[2] K. Hui and A. N. Berker, Phys. Rev. Lett. **62**, 2507 (1989).
[3] M. Aizenman and J. Wehr, Phys. Rev. Lett. **62**, 2503 (1989).
[4] J. Cardy and J. L. Jacobsen, Phys. Rev. Lett. **79**, 4063 (1997); J. L. Jacobsen and J. Cardy, Nucl. Phys. B **515**, 701 (1998).
[5] K. Uzelac, A. Hasmy, and R. Jullien, Phys. Rev. Lett. **74**, 422 (1995).
[6] H. G. Ballesteros, L. A. Fernández, V. Martín-Mayor, A. Muñoz Sudupe, G. Parisi, and J. J. Ruiz-Lorenzo, Phys. Rev. B **61**, 3215 (2000).
[7] C. Chatelain, B. Berche, W. Janke, and P. E. Berche, Phys. Rev. E **64**, 036120 (2001).
[8] M. Hellmund and W. Janke, Phys. Rev. E **67**, 026118 (2003).
[9] J. Q. Yin, B. Zheng, and S. Trimper, Phys. Rev. E **72**, 036122 (2005).
[10] M.-T. Mercaldo, J.-Ch. Anglès d'Auriac, and F. Iglói, Phys. Rev. E **73**, 026126 (2006).
[11] L. A. Fernández, A. Gordillo-Guerrero, V. Martín-Mayor, and J. J. Ruiz-Lorenzo, Phys. Rev. Lett. **100**, 057201 (2008).
[12] A. B. Harris, J. Phys. C **7**, 1671 (1974).
[13] F. Y. Wu, Rev. Mod. Phys. **54**, 235 (1982).
[14] R. J. Baxter, J. Phys. C **6**, L445 (1973).
[15] S. Chen, A. M. Ferrenberg, and D. P. Landau, Phys. Rev. Lett. **69**, 1213 (1992).
[16] S. Wiseman and E. Domany, Phys. Rev. E **51**, 3074 (1995).
[17] S. Chen, A. M. Ferrenberg, and D. P. Landau, Phys. Rev. E **52**, 1377 (1995).
[18] A. W. W. Ludwig, Nucl. Phys. B **330**, 639 (1990).
[19] V. Dotsenko, M. Picco, and P. Pujol, Nucl. Phys. B **455**, 701 (1995).
[20] T. Olson and A. P. Young, Phys. Rev. B **60**, 3428 (1999).
[21] C. Chatelain and B. Berche, Phys. Rev. Lett. **80**, 1670 (1998).
[22] R. Paredes V. and J. Valbuena, Phys. Rev. E **59**, 6275 (1999).
[23] C. Chatelain and B. Berche, Phys. Rev. E **58**, R6899 (1998).
[24] C. Chatelain and B. Berche, Phys. Rev. E **60**, 3853 (1999).
[25] J. Q. Yin, B. Zheng, and S. Trimper, Phys. Rev. E **70**, 056134 (2004).
[26] J. Cardy, Physica A **263**, 215 (1999).
[27] M. Picco, e-print arXiv:cond-mat/9802092.
[28] H. K. Janssen, K. Oerding, and E. Sengespeick, J. Phys. A **28**, 6073 (1995).
[29] K. Oerding and H. K. Janssen, J. Phys. A **28**, 4271 (1995).
[30] S. Chen and D. P. Landau, Phys. Rev. E **55**, 40 (1997).
[31] C. Deroulers and A. P. Young, Phys. Rev. B **66**, 014438 (2002).
[32] Z. Q. Pan, H. P. Ying, M. L. Chen, and D. W. Gu, Commun. Theor. Phys. **37**, 745 (2002).
[33] H. P. Ying and K. Harada, Phys. Rev. E **62**, 174 (2000).
[34] R. H. Swendsen and J.-S. Wang, Phys. Rev. Lett. **58**, 86 (1987).
[35] C. F. Baillie and P. D. Coddington, Phys. Rev. B **43**, 10617 (1991).
[36] S. Tang and D. P. Landau, Phys. Rev. B **36**, 567 (1987).
[37] M. Suzuki, Prog. Theor. Phys. **51**, 1992 (1974).
[38] S. Fan and F. Zhong, Phys. Rev. E **76**, 041141 (2007).
[39] D. S. Fisher, Phys. Rev. Lett. **56**, 416 (1986).
[40] K. G. Wilson, Rev. Mod. Phys. **55**, 583 (1983).
[41] S. K. Ma, Phys. Rev. Lett. **37**, 461 (1976).
[42] R. H. Swendsen, Phys. Rev. Lett. **42**, 859 (1979).
[43] J. Tobochnik, S. Sarker, and R. Cordery, Phys. Rev. Lett. **46**, 1417 (1981).
[44] S. L. Katz, J. D. Gunton, and C. P. Liu, Phys. Rev. B **25**, 6008

(1982).
[45] F. Zhong, Phys. Rev. B **66**, 060401(R) (2002).
[46] F. Zhong and Z. F. Xu, Phys. Rev. B **71**, 132402 (2005).
[47] F. Zhong, Phys. Rev. E **73**, 047102 (2006).
[48] F. Zhong, J. Dong, and D. Y. Xing, Phys. Rev. Lett. **80**, 1118 (1998).
[49] W. Kinzel and E. Domany, Phys. Rev. B **23**, 3421 (1981).
[50] J. T. Chayes, L. Chayes, D. S. Fisher, and T. Spencer, Phys. Rev. Lett. **57**, 2999 (1986).
[51] See, e.g., S. K. Ma, *Modern Theory of Critical Phenomena* (Benjamin, Reading, MA, 1976).
[52] H. G. Ballesteros, L. A. Fernández, V. Martín-Mayor, A. Muñoz Sudupe, G. Parisi, and J. J. Ruiz-Lorenzo, Phys. Rev. B **58**, 2740 (1998).
[53] M. E. Fisher and M. Randeria, Phys. Rev. Lett. **56**, 2332 (1986).